Original Paper

Synthesis, Spectroscopic, Calculated and Thermal Study of Copper and Cobalt Complexes with Dacarbazine

Grzegorz Świderski[1,*], Ryszard Lazny[2], Michał Sienkiewicz, Monika Kalinowska[1], Renata Swislocka[1], Ali Osman Acar[3], Aleksandra Golonko[4], Marzena Matejczyk[1] and Włodzimierz Lewandowski[1,*]

1   Department of Chemistry, Biology and Biotechnology, Bialystok University of Technology, Wiejska Street 45E, 15-351 Bialystok

2   Institut of Chemistry, University of Bialystok, Ciolkowskiego Street 1K, 15-245 Bialystok

3   Micro and Nanotechnology, TOBB University of Economics and Technology, Ankara, Turkey

4   Institute of Agricultural and Food Biotechnology, Rakowiecka 36, 02-532 Warsaw, Poland

*   Correspondence: g.swiderski@pb.edu.pl; w.lewandowski@pb.edu.pl

Abstract: Dacarbazine, DAC, 5-(3,3-dimethyltriazeno)imidazol-4-carboxamideis is an imidazole-carboxamide derivative, that is structurally related to purines. DAC belongs to the triazene compounds, which are a group of alkylating agents with antitumour and mutagenic properties. DAC is a non-cell cycle specific drug, active on all phases of cellular cycle. In the frame of this work the 3d-metal complexes (cobalt and copper) with dacarbazine were synthesized. Their spectroscopic properties by the use of FT-IR, FT-Raman and ^{1}HNMR were studied. The structures of dacarbazine and its complexes with copper(II) and cobalt(II) were calculated using DFT methods. The effect of metals on the electronic charge distribution of dacarbazine was discussed on the basis of calculated NBO atomic charges. The reactivity of metal complexes in relation to ligand alone was estimated on the basis of calculated energy of HOMO and LUMO orbitals. The aromaticity of imidazole ring in dacarbazine and the complexes was compared (on the basis of calculated geometric indices of aromaticity). Thermal stability of the investigated 3d-metal complexes with dacarbazine and the products of their thermal decomposition were analyzed.

Keywords: dacarbazine, triazene, anticancer properties, 3d-metal complexes, spectroscopy (IR, Raman), NMR

1. Introduction

Dacarbazine (DAC) [5-(3,3-Dimethyl-1-triazenyl) imidazole-4-carboxamide]belongs to the alkylating agents of triazene group use in anticancer therapy [1-4]. DAC is an imidazole-carboxamide derivative, that is structurally related to purines. DAC is a non-cell cycle specific drug, active on all phases of cellular cycle. This drug is used for chemotherapy in different types of cancer malignant melanoma, soft-tissue sarcoma, osteogenic sarcoma, neuroblastomas and Hodgkin's disease [5-6]. The detailed molecular mechanism of DAC activity is unclear. Research to date indicates three possible mechanisms of action of this drug: (a) inhibition of DNA synthesis by acting as a purine analogue, (b) action as alkylating agent, (c) interaction with SH groups [7]. Hayward et al., 1984 propose another mechanism of DAC activity based on antimetabolite-like activity. In

this mechanism, DAC plays the role of an inhibitor of purinic base incorporation into DNA during DNA synthesis. However, this mechanism does not seem to play a key role in the antitumour activity of DAC [8].

Based on experimental data it seems, that alkylation of nucleic acid is primary mode of antitumour DAC action [7]. DAC as alkylator donates of methyl groups to many sites in DNA. A very common place of attack of DAC is O(6)-position of guanine resulting in O(6)-methylguanine (O(6)-MeG) that frequently mispairs with thymine during DNA duplication. Each cell is equipped with repair systems, mismatch repair (MMR) system recognizes O(6)-MeG:T mismatches that leads to cell cycle arrest and cell death. If MMR is defective, the cell will divide and GC → AT transition mutations occur (Fig. 1.) [5-6]. Generally, DAC causes DNA damage, cell cycle arrest and apoptosis [9]. Hayward et al., 1984 propose another mechanism of DAC activity based on antimetabolite-like activity. In this mechanism, DAC plays the role of an inhibitor of purinic base incorporation into DNA during DNA synthesis. However, this mechanism does not seem to play a key role in the antitumour activity of DAC [8]. DAC is a prodrug that is activated by N-demethylation in liver microsomes with participation of the liver's microsomal enzymes (CYP1A1,CYP1A2, and CYP2E1) that hydroxilate and N-demethylate the DAC [7].
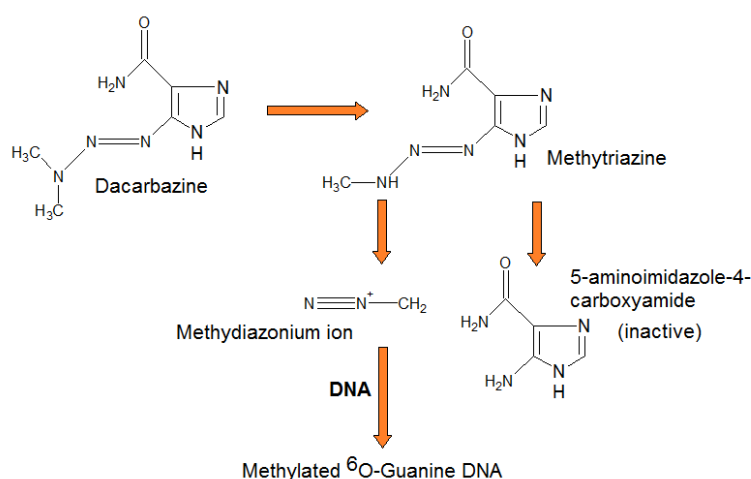

Figure 1. Mechanism of action of dacarbazine

Studies by earlier authors have shown that DAC, in combination with other drugs is used for treating renal adenocarcinoma, soft tissue sarcoma and malignant lymphomas. Al-Qatati and Aliwaini 2017 in their work presented that combined pitavastatin with DAC treatment induces cell death through intrinsic apoptosis in melanoma cells [9]. Naserian et al., 2018 investigated the cytotoxicity and apoptosis of the metformin alone and in combination with DAC in Raji and Ramos lymphoma cell lines [10]. Metformin showed synergistic cytotoxic effects in combination with DAC, reduced cell viability, and increased apoptosis in Raji and Ramos lymphoma cells in comparison with the use of each drug alone. Additionally, Finotello et al., 2015 reported that results of *in vitro* and *in vivo* studies suggest that dacarbazine acts synergistically with anthracyclines and has a moderate effect on the treatment of high-grade sarcomas in humans [11].

The greatest obstacle in the treatment of patients with advanced stage of melanoma and other cancers is the unique tumor resistance, both primary and secondary, to all known compounds including dacarbazine. The complexation of metal ions with anticancer drugs creates the possibility of an increase in the bioavailability and activity of drugs [12,13]. Metal complexes play a very important role in modern cancer therapy. The complexation of metal ions with biologically active ligands, can change their therapeutic activity. Metal ions affect the distribution of the electronic system of ligands what in turn changes the reactivity   and biological activiry of the ligands [14,15]. Complexes with some of the transition metals, e.g. Au, Ag, Co, Cu, Ni, Fe Pt(II) and (IV), Pd(II) and Ru(III) show high anticancer activity [16].

DAC possesses triazene group connected to the imidazole ring which is attached to carboxamide group. In the structure of the DAC, they are atoms that may be donors of electron pairs, making possible complexation of the ligand with metal ion. Different types of metal-ligand complex can be formed when the molecule of dacarbazine coordinates metal through seven potential donor atoms.

Several studies have shown that complexation of dacarbazine with metal ions may change the reactivity and stability of the molecule, thereby improving its therapeutic properties. In vitro and in vivo studies have shown that iron (III) complex of dacarbazine may exhibit increased anti-tumor effect compared to the ligand alone [17-18]. Yassien and Hossieny 2014 in their work investigated the influence of DAC complexation with Cu(II) on the drug intercalation to DNA. The results of that experiments showed that the interaction of DAC with dsDNA in the presence of Cu(II) led to a much stronger intercalation, comparable to DAC alone [19].

Our studies showed that there is a dependency between the electronic charge distribution in metal complex and salt molecules and the location of these metals in the periodic table [20]. Alkali metal cations and some heavy metal cations [Ag(I), Pb(II), Hg(I), Hg(II)] perturb the electronic system of ligands (benzoic, salicylic, pyridinecarboxylic acids and others), whereas 3d and 4f metal cations stabilize it [21-26]. This conclusion allows to foresee the changes in the electronic structure under the influence of metal cations and estimation of the physicochemical and biologically properties of complexes.

In the frame of this work the 3d-metal complexes with dacarbazine were synthesized. The aim of the work was to estimate the effect of metal ions (copper(II) and cobalt(II)) on the reactivity and electronic stability of dacarbazine. For this purpose, the spectroscopic properties of compounds was studied by the use of FT-IR, FT-Raman and   ^{1}HNMR. Thermal stability of the investigated 3d-metal complexes (cobalt(II) and copper(II)) with dacarbazine and the products of their thermal decomposition was analyzed.

2. Materials and Methods

2.1. Synthesis

Complexes dacarbazine - $CoCl_2$ $(DAC)_2*1,75CH_3OH$ and $CuCl_2(DAC)_2*1,5CH_3OH$ obtained by the same method of synthesis by reaction dacarbazine of metal chlorides in a methanolic medium. The weight amount of dacarbazine (0.2   mol)   was   dissolved in   cold   methanol   and   it   was   added   to   5   ml   of   methanolic   solution

of metal chloride (0,1 mol) ($CuCl_2$, $CoCl_2$). Then the mixture was shaken for 2 h in the water bath in room temperature. Next 50 ml of diethyl ether was added and it was left for 2 h. The precipitate was washed three times with 50 ml of diethyl ether. The obtained complexes were dried in vacuum.

Elemental analysis: Anal. Calc. for $CoCl_2(DAC)_2*1.75CH_3OH$: C, 29.62; H, 4.75; N, 30.72. Found: C, 29.35; H, 5.03; N, 30.318. Calc. for $CuCl_2(DAC)_2*1.5CH_3OH$: C, 29.98 ; H, 4.91; N, 30.53. Found: C, 30.13; H, 5.30; N, 30.82.

1.1. Methods

The FT-IR spectra were recorded with an Alfa (Bruker) spectrometer within the range of 400–4000 cm^{-1}. Samples in the solid state were measured in KBr matrix pellets and ATR technique. FT-Raman spectra of solid samples were recorded in the range of 100–4000 cm^{-1} with a MultiRam (Bruker) spectrometer. The resolution of the spectrometer was 1 cm^{-1}. The ^1H spectra of DMSO solution of studied compounds were recorded with a Bruker Avance II 400 MHz unit at room temperature. TMS was used as an internal reference. Elemental analysis for the weight percentages of carbon and hydrogen was done with Perkin-Elmer 240 equipment. To calculate optimized geometrical structures, NMR and IR spectra, NBO analysis, HOMO/LUMO orbitals of dacarbazine and complexes with copper and cobalt was used density functional (DFT) hybrid method B3LYP with non-local cor-relation provided by Lee–Young–Parr expression. All calculations were carried out with 6-311++G(d,p) basis set and performed with GAUSSIAN 09 [27] packed.

The aromaticity indices (HOMA, GEO, EN, I6) were calculated for geometric structures (theoretical and calculated) of dacarbazine and it complexes. The HOMA index (harmonic oscillator model of aromaticity) differs from all other geometry-based ones by assuming another reference bond length. In this model, instead of the mean bond length a concept of the optimal bond length is applied [28]:

$$HOMA = 1 - \left[\alpha (R_{opt} - R_{av})^2 + \frac{\alpha}{n} \sum (R_{av} - R_i)^2 \right] = 1 - EN - GEO$$

Within the confines of the HOMA model, it is possible to obtain two components which describe different contribution to decrease in aromaticity, i.e. (a) due to bond elongation (the EN component), and (b) due to bond length alternation (the GEO component). The value of HOMA index is equal 1 for the entire aromatic system; HOMA = 0 when structure is non-aromatic and HOMA < 0 for anti-aromatic ring.

The value of the Bird's aromaticity index (I_5, I_6) describes the equation [29]:

$$I = 100 \{ 1 - (V / V_k) \}$$

where: V_k is for the five-membered rings 35 and the six-membered 33.3, and V is calcu-lated from the equation:

$$V = (100 / n_{av}) \left[\sum_{r=1}^{n} (n_r - n_{av})^2 / n \right]^{\frac{1}{2}}$$

where: n_{av} - average binding order, n - bond order based on bond length: n = (a / R) - b, a and b - parameters depending on the type of atoms in the bond.

NBO analysis was performed for the optimized structures to determine the electronic charge distribution [30]. Calculations were made using the B3LYP/6-311++G(d, p) method.

Thermal analyses of the prepared complexes were performed by the thermogravimetric (TG) methods using the Perkin Elmer analyser. The products of dehydration and decomposition processes were determined from the TG curves. The TG measurement has been performed in temperature range 50°C-890°C in air atmosphere.

The crystal structure of the DNA dodecamer was obtained from Protein Database (PDB ID: 1BDNA) and used for molecular modeling studies carried out in AutoDock 4.2 MGL Tools package supplied with AutoGrid4.0 and AutoDock4.0 [31]. In order to analyze the obtained results and compare the number of hydrogen bonds formed, the VMD (Visual Molecular Dynamics) program was used [32].

AutoGrid4.0 was used to compute grid maps using a grid box. The molecular docking was carried out by setting the grid box size to cover the predicted binding sites, using 52, 56, 118 x, y, z points with a grid spacing of 0,375 Å. The grid center was set to 14.72, 21.006, 8.801 x,y and z dimensions respectively. The Lamarckian genetic algorithm (LGA) was selected to generate the best ligand conformers. We performed successfully 1000 docking runs with AutoDock4.0 for each ligands (DAC1, DAC2) and Co(II)-DAC, Cu(II)-DAC complexes. As standard values for hydrogen bond formation assumed distance 2,9 Å and cutoff angle 60 degree (120 to 180 degrees). To visualize results BIOVIA Discovery Studio and USCF Chimera 1.10.2were used [33,34].

2. Results and discussion

2.1. IR and Raman spectra

The IR and Raman spectra of dacarbazine and IR spectra of cobalt (II) and copper (II) complex of dacarbazine were shown in Fig. 2.
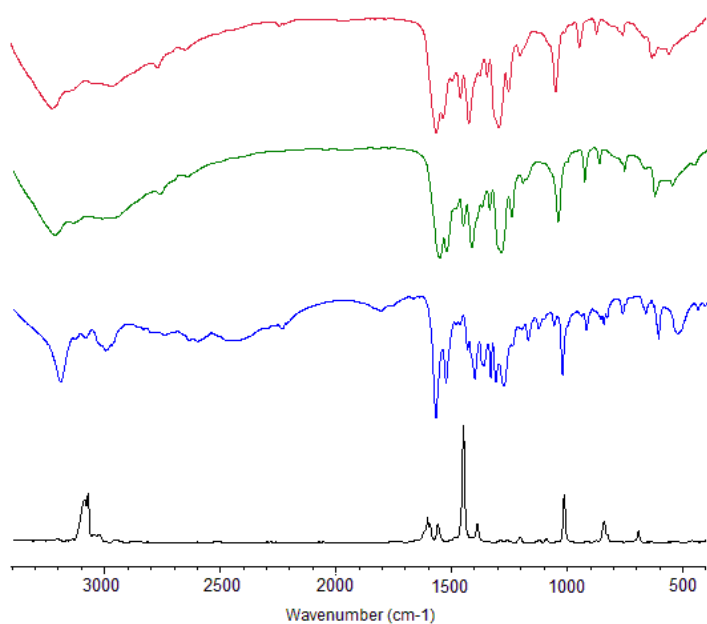
Figure 2. IR spectra of dacarbazine (blue line), cobalt complex (red line), copper complex (green line) and Raman spectra of dacarbazine (black line).

The wavenumbers and intensities of selected bands from the experimental and theoretical IR and Raman spectra of ligand and experimental IR spectra of complexes were gathered in Table 1. The assignment of bands was done on the basis of theoretical wavenumbers obtained at the B3LYP/6-311++G** level as well as literature data [35]. The theoretical wavenumbers were scaled to reproduce adequately the experimental *wavenumbers (*f=0.967). Some characteristic bands occurred in experimental the spectra of dacarbazine, i.e. bands assigned to the stretching vibrations of the carbonyl group νC=O at 1609 cm^{-1} (IR) and 1604 cm^{-1} (Raman). The theoretical wavenumbers of the νC=O band were 1691 cm^{-1} (for the DAC1 conformer) and 1683 cm^{-1} (in the case of the DAC2 conformer) (Fig. 3)   (the values scaled by the factor f=0.967). In the IR spectra of Co (II) and Cu (II) complexes of dacarbazine the νC=O band was of similar wavenumbers and reduced intensities compared with the spectra of ligand (i.e. 1605 cm^{-1} - Co (II) complex and 1609 cm^{-1} - Cu (II) complex). This suggested that the carbonyl group did participate in metal ion coordination. In the spectra of dacarbazine and its metal complexes the characteristic bands assigned to the vibrations of NH_2 (of amide group) occurred. There were bands of the stretching asymmetric vibrations $\nu_{as}NH_2$ located at 3383 cm^{-1} (IR) and 3371 cm^{-1} (Raman) as well as stretching symmetric vibration $\nu_s NH_2$ near 3269 cm^{-1} (IR). In the spectra of complexes, the bands assigned to the stretching vibrations $\nu_{as}NH_2$ were significantly shifted whereas bands of $\nu_{as}NH_2$ disappeared compared with the appropriate bands in the spectra of ligand. Significant changes were also observed in the case of deforming out-of-plane vibrations of NH_2 group (ϱNH_2), i.e. 1436 cm^{-1} – in the spectrum of ligand, 1440 cm^{-1} – Cu and Co complexes as well as 542 cm^{-1} – ligand and 565 cm^{-1} – Co complex, 568 cm^{-1} Cu complex. The metal complexation affected the location of the band derived from the vibrations of the C-NH_2 group as well. Namely, the band of deforming out-of-plane vibrations ϱC-NH_2 were located at 1476 cm^{-1} and underwent movement to the 1487 cm^{-1} and 1488 cm^{-1} in the cobalt and copper complexes of dacarbazine, respectively. The characteristic changes in the wavenumbers of the bands assigned to the vibrations of N=N-N and CH_3 groups were observed.

Table 1. The wavenumbers from the IR (theoretical and experimental) and Raman spectra of dacarbazine and IR spectra of dacarbazine complexes with cobalt and copper

| Calculated IR (B3LYP 6-311G(d,p) | | | | | | Experimental spectra [cm^{-1}] | | | | |
| DAC 1 | | | DAC 2 | | | DAC | | Cobalt complex | Copper complex | |
Unscaled	Scaled = 0.967	Intensity	Unscaled	Scaled =0.967	intensity	IR	Raman	IR	IR	Assignments
3703	3581	105.50	3728	3605	72.84	3383 s	3371 w	3406 s	3406 s	$\nu_{as}NH_2$
3647	3527	58.23	3560	3443	65.93	-	-	3322 s	-	νNH
3549	3432	60.67	3585	3467	53.44	3269 m	-	-	-	$\nu_s NH_2$
3238	3131	2.26	3240	3133	2.09	3174 m	-	3188 s	3186 s	νCH_{ar}
3144	3040	7.76	3143	3039	11.28	3147 m	3141 vw	-	-	$\nu_s CH_3$
3139	3035	8.76	3139	3035	5.32	2964 m	-	-	-	$\varrho_s CH$
3085	2983	13.51	3097	2995	15.07	2905 m		2925 m	2923 m	$\nu_{as} CH_3$
3078	2976	26.13	3074	2973	28.84	2793 m	-	-	2796 w	$\nu_{as} CH_3$
3014	2915	47.62	3021	2921	40.93	2753 m	-	-	-	$\nu_s CH_3$
3003	2904	78.48	2997	2898	94.76	2612 m	-	-	-	$\nu_s CH_3$
1749	1691	494.07	1740	1683	326.18	1609 vs	1604 w	1605 s	1609 s	$\nu C=O$
-	-	-	-	-	-	1656 vs	-	1637 vs	1639 vs	νCH_3
1620	1567	141.69	1607	1554	256.98	-	-	-	-	$\varrho C-NH_2$
-	-	-	-	-	-	1561 w	1559 w	1561 m	1566 m	$\varrho_s CH_3$
1569	1517	3.59	1586	1534	55.59	1510 m		1525 s	1528 s	νCN
1527	1477	197.90	1525	1475	155.81	1476 s	1488 vw	1487 vs	1488 vs	$\varrho C-NH_2$
1483	1434	27.90	1481	1432	25.74	1436 m	1449 vs	1440 m	1440 m	ϱNH_2
1451	1403	75.22	1453	1405	32.35	1402 s	-	1405 m	1405 m	$\nu CC, \nu_{ring}, \varrho NH_2$
1438	1391	5.80	1438	1391	9.68	-	-	-	-	$\nu CC, \alpha N-CH2, \beta NCH$
1431	1384	47.98	1430	1383	74.13	1381 s	1388 w	-	-	$\beta_{as} CH_3, \nu_{ring}$
1389	1343	21.23	1388	1342	24.58	1344 s	-	1352 vs	1351 vs	$\beta_s CH_3, \nu_{ring}$
1363	1318	114.39	1367	1322	408.84	1304 m	-	1306 s	1307 s	$\beta_s CH_3, \nu_{ring}$
1331	1287	36.74	1328	1284	40.87	1270 w	1289 vw	-	-	$\beta_s CH_3, \nu_{ring}, \beta NCH$
1270	1228	2.30	1260	1218	16.53	1259 w	1258 vw	1253 vs	1255 m	$\nu CN, \beta CH$

1231	1190	67.15	1233	1192	20.71	1231 m	1204 vw	-	-	ν_{ring}, βCH
1153	1115	25.50	1152	1114	39.12	1183 w	-	-	-	$\beta CH + \nu NN$
1136	1099	26.51	1137	1099	9.08	1072 s	1091 vw	1091 s	1091 s	νNN, βCH
1114	1077	24.06	1110	1073	7.62	-	-	-	-	$\beta CH + \beta CNC$
1091	1055	202.22	1093	1057	17.91	1049 w	1012 m	-	-	ϱCH_2, βCH
1084	1048	12.72	1075	1040	117.70	986 w	-	-	-	$\varrho C\text{-}NH_2$, βCNC
1062	1027	14.22	1061	1026	18.40	962 w	-	969 m	980 w	ϱCH_2, βCNC
951	920	4.32	955	923	15.06	904 w	913 vw	902 w	902 w	ϱCH_3, βCH
915	885	14.86	912	882	16.25	896 w	-	-	-	ϱCH_3, ν_{ring}
817	790	9.74	812	785	5.02	882 w	-	-	-	$\Delta ring$, $\nu_{ring}(CN)$
799	773	2.21	799	773	2.40	868 w	873 vw	-	-	ϱCH_3, ν_{ring}
797	771	10.95	798	772	14.79	796 w	-	-	-	βNCH, βNCC
672	650	13.44	683	660	14.27	690 w	691 w	-	-	βNH, βCCO
668	646	0.82	679	657	0.01	653 vw	-	-	-	$\beta(CCN + NH)$
632	611	25.62	602	582	43.51	630 m	-	646 m	649 m	αNNN, αCNC
586	567	0.50	596	576	0.65	542 m	-	565 m	568 m	ϱNH_2, αNNH, αCCO
552	534	73.21	574	555	104.33	450 w	445 vw	-	-	$ring_{def}$
550	532	39.82	568	549	10.64	-	-	-	-	$ring_{def}$
447	432	10.01	449	434	11.86	416 vw	-	-	-	$\alpha C\text{-}NH_2$

* Abbreviation: band intensity s – strong, m – medium, w – weak, vw – very weak, type of vibrations: ν – stretching, ϱ-bending out-of-plane β – bending in-plane, α- deformation in-plane, Δ-deformation out-of-plane, ring_def-deformation of ring, s-symmetric, as-asymmetric

Dacarbazine crystal structure

Dacarbazine DFT calculated
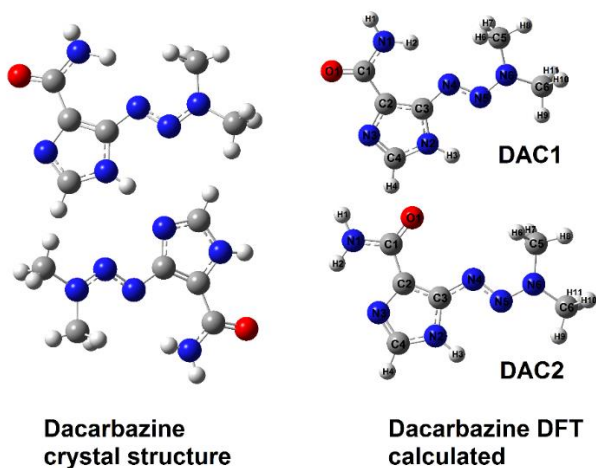
Figure 3. Crystal (A) and theoretical structure (B3LYP/6-311++g(d,p) of dacarbazine

The band assigned to the deformations of the triazene group αNNN was located at 630 cm^{-1} in the spectra of ligand, and then was shifted toward higher wavenumbers in the spectra of complexes (649 cm^{-1} – Cu complex and 646 cm^{-1} – Co complex). The symmetric stretching vibrations of the methyl group ν_sCH$_3$, which were present in the spectra of ligand at 3147, 2946, 2753 and 2612 cm^{-1}, disappeared in the spectra of metal complexes. Whereas band of asymmetric stretching vibrations of the methyl group ν_sCH$_3$ were significantly shifted in the spectra of complexes comparing with the spectra of ligand, i.e. 2905 cm^{-1} – in the IR spectra of dacarbazine and 2925 cm^{-1} and 2923 cm^{-1} in the IR spectra of Co and Cu complexes, respectively. The band of the deforming in-plane vibrations of the methyl group of dacarbazine, disappeared or decreased/ increased in their wavenumbers in the spectra of Cu and Co complexes (Table 2).

Table 2. The chemical shifts [ppm] from the ^{1}HNMR theoretical (GIAO/B3LYP/6-311++G**) and experimental spectra of dacarbazine and experimental spectra of cobalt and copper complexes with dacarbazine

		DAC 1	DAC 2	Dacarbazine complexes	
				cobalt	copper
H (amide group)	Exp.	7.30, 7.42	-	7.44, 7.56	-
	Theoret.	6.86, 4.57	6.87, 4.40	8.94, 6.38	8.29, 5.42
H (CH$_{ring}$)	Exp.	7.51	-	7.68	-
	Theoret.	7.20	6.98	8.90	7.74
H (NH$_{ring}$)	Exp.	9.52	-	9.71	-
	Theoret.	8.56	8.72	9.43	8.81
H (CH$_3$-triazene group)	Exp.	3.14	-	3.02	-
	Theoret.	3.67, 3.48, 3.36, 3.19 2.29, 2.59	4.73, 4.37, 3.91, 3.88 3.69, 3.17	3.78, 3.74, 3.71, 3.44	3.62, 3.61, 3.61, 3.24

Moreover, the coordination of copper (II) and cobalt (II) by dacarbazine caused changes in the spectra of complexes in the region of bands assigned to the stretching (ν_{ring}) and deforming (ring$_{def}$) vibrations of the ring (comparing with the appropriate bands in the spectra of dacarbazine). Namely, ν_{ring} bands located at 1381, 1270, 1231 cm^{-1} and ring$_{def}$

bands near 882 and 450 cm^{-1} disappeared in the spectra of metal complexes. Whereas ν_{ring} bands situated in the spectra of ligand at 1344 and 1402 cm^{-1} were slightly shifted to the higher wavenumbers in the spectra of complexes. The band of stretching vibrations of the CH bond of the aromatic ring of dacarbazine located at 3174 cm^{-1} was shifted toward higher wavenumbers in the spectra of complexes (i.e. 3188 cm^{-1} – Co (II) complex and 1386 cm^{-1} – Cu (II) complex). The deforming vibrations of CH bond of the ring slightly moved to the higher wavenumbers in the spectra of complexes comparing with the spectra of ligand.

The difference between the location of the appropriate bands in the spectra of dacarbazine and copper (II) and cobalt (II) complexes of dacarbazine might be caused by the coordination of metal ions by the oxygen atom of carbonyl group and nitrogen atom of imidazole ring.

2.2. NMR spectra

In the experimental 1HNMR spectra of dacarbazine four groups signals from protons were observed (Table 2). The values of the chemical shift for two protons of amide group have been values   7.42 and 7.30 ppm. This signals possessed very low intensity in the spectra of cobalt complex, and was unsignificantly shifted to 7.44 and 7.56 ppm. In the spectra of ligand the signals at 2.29-3.67 ppm was assigned to the protons of the methyl group.   Complexation of dacarbazine by the cobalt caused unsignificantly displacement of this signals. On the basis of the value of signals deriving from the aromatic protons (imidazole ring) the effect of metal ions on the electronic charge distribution of ligand might be discussed. The movement of the chemical shifts of aromatic protons toward higher wavenumbers showed the increased in the aromaticity of the ring as well as the stabilization of the aromatic system [20]. In the case of cobalt (II) complexes of dacarbazine, it was observed the slight increased in the value of the chemical shift of proton of CH bond of the aromatic ring as well as the increased of the chemical shift of NH proton of the aromatic ring.   Proton NMR spectrum for copper complex could not be recorded. The theoretically calculated chemical shifts in the proton spectrum of the copper complex show similar trends in proton shifts relative to the ligand as in the cobalt complex. Cobalt and copper   possessed stabilizing effect on the electronic system of ligand. The same effect was observed on the basis of the IR spectra of Co and Cu complexes of dacarbazine (an increased in the values of the wavenumbers and intensities of the aromatic ring). Our long-term study on the influence of metals on the electronic system of ligand (aromatic and heteroaromatic system of five- and six-membered carboxylic acids) showed that 3d transition metals (including cobalt and copper) stabilize the electronic system of ligands [20-24]. In the spectra of such complexes (a) an increase in the values of signals of the aromatic protons (in 1HNMR spectra), and (b) an increase in wavenumbers and intensity of bands assigned to the aromatic system (in the IR spectra) comparing with the appropriate signals/bands in the spectra of ligand were observed.

2.3. Structure, aromaticity and NBO analysis of dacarbazine and copper and cobalt complexes

The dacarbazine molecule has a triazene moiety linked to an imidazole ring. IR, NMR studies and literature X-ray data on the structure of dacarbazine complexes [36] showed that metals such as copper and cobalt coordinate the ligand (dacarbazine) through the carbonyl group and the nitrogen atom from the imidazole ring. A similar type of metal-ligand coordination has been observed for 3d-transition metal complexes with imidazole carboxylic acid [38]. On the basis of spectroscopic studies (IR, Raman) and theoretical calculations, it was found that 3d metals affect the electronic charge distribution of the aromatic ring of ligand. With the increase in the electronic stability of the ligand, the reactivity of the compound changes, which is important in the case of biologically active ligands. Theoretical structures of dacarbazine complexes with cobalt and copper were calculated. The calculated bond lengths and the values of the selected angles were compared with these one obtained for experimentally solved structures (X-ray) available in the literature. The geometric indices of aromaticity (HOMA, GEO, EN and I5) and the electronic charge distribution by the NBO method   were also calculated. Figure 3 shows the experimentally determined structure [36] and the calculated two dacarbazine conformers (at B3LYP method). The figure 4 shows the experimental structure of the complex of copper with dacarbazine (A) [37] and the theoretically modeled structures of the complexes with copper (B) and cobalt (C).

Both theoretically modeled dacarbazine conformational structures have similar energy values. According to the calculated geometric aromaticity indices, the imidazole ring of the DAC1 structure is more stable than the DAC2 structure (Table 3). The system is stabilized by an intramolecular hydrogen bond between the hydrogen atom of the amino group and the nitrogen atom of the triazene group. The length of this bond is 2.154 Å. In the DAC2 structure, the amide moiety is rotated 180° along the C1-C2 carbons as compared to the DAC1 structure. The aromatic system of imidazole in this structure is less stable, as evidenced by the values of the aromaticity indices. The structure of the DAC1 monomer is the same as that of experimentally determined dacarbazine. In the structure determined by the X-ray diffraction method [32] there is an intramolecular hydrogen bond that stabilizes the aromatic system between the hydrogen atom of the amino group and the triazene nitrogen atom with a length of 2.294 Å, and an intermolecular hydrogen bond with a length of 1.945 Å. The values of geometric aromaticity indices calculated for the experimental structure and the theoretically modeled DAC1 are at a similar level (Table 3). The differences in the lengths of the corresponding bonds in the experimentally determined dacarbazine structure and the theoretically modeled DAC1 monomer range from 0.001 to 0.026 Å.

Table 3. Geometrical aromaticity parameters and selected bond lengths and angle values obtained for dacarbazine and copper(II) and cobalt(II) complexes of dacarbazine

	Dacarbazine			Copper complex		Cobalt complex
	Exp [36]	DAC1	DAC2	Exp [37]	Calc	Calc
Energy	-	-638.54	-638.54	-	-3199.60	-2941.88
Dipole m	-	10.7498	5.5647	-	21.8411	22.5754

Aromaticity indices						
HOMA	0.905	0.893	0.880	0.925	0.897	0.890
GEO	0.060	0.069	0.079	0.057	0.065	0.067
EN	0.035	0.039	0.041	0.017	0.039	0.043
I5	67.97	67.39	65.35	70.44	68.42	67.68
Bond lengths [A]						
C1-O1	1.230	1.218	1.222	1.362	1.236	1.247
C1-N1	1.338	1.370	1.366	1.309	1.345	1.342
C1-C2	1.470	1.492	1.484	1.460	1.477	1.465
C2-C3	1.379	1.392	1.388	1.387	1.393	1.392
C3-N2	1.375	1.377	1.381	1.370	1.383	1.381
N2-C4	1.352	1.370	1.367	1.345	1.356	1.359
C4-N3	1.333	1.307	1.309	1.311	1.311	1.312
N3-C2	1.387	1.376	1.383	1.379	1.379	1.384
C3-N4	1.383	1.384	1.380	1.387	1.382	1.380
N4-N5	1.285	1.270	1.279	1.286	1.273	1.274
N5-N6	1.304	1.325	1.326	1.299	1.314	1.313
N6-C5	1.451	1.456	1.458	1.450	1.455	1.455
N6-C6	1.449	1.453	1.451	1.450	1.458	1.458
Angles [º]						
N2-C3-N4	127.50	125.36	125.07	116.37	115.48	116.15
C3-N4-N5	112.80	113.71	113.23	112.17	115.88	115.46
N4-N5-N6	113.42	115.20	114.26	114.66	114.71	114.64
N5-N6-C6	116.55	115.90	116.01	122.46	121.71	121.70
C5-N6-C6	120.96	120.43	120.46	120.31	120.82	120.76
C1-C2-N3	120.18	120.93	121.18	112.88	113.31	112.19
O1-C1-N1	123.28	122.53	123.17	121.95	122.79	122.19

104

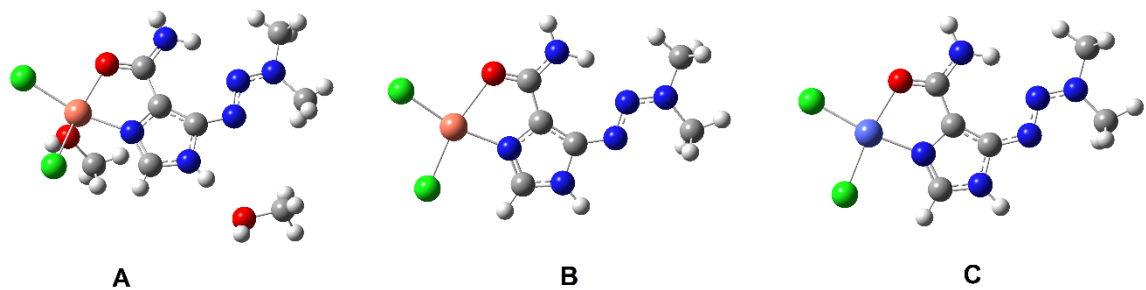**A**   **B**   **C**

105

Figure 4. Crystal (A), theoretical structure (B3LYP/6-311++g(d,p) of cobalt (B) and Copper (C) complex with dacarbazine

106
107

The complexation of dacarbazine with 3d transition metals (copper and cobalt) influences the stability of the ligand's electronic system, which is observed by changing the aromaticity of the system expressed in the values of aromaticity indices, changes in the

108
109
110

distribution of electronic charge and changes in the bond lengths in the studied systems. 111
The comparison of the structure of the dacarbazine complex with copper [37] to 112
dacarbazine [36] shows that the aromatic system of the imidazole ring is stabilized by 113
complexation (Table 3). It was observed both when comparing the ligand structure to the 114
complex for the experimental and theoretically modeled structures (the effect of the metal 115
is more noticeable when comparing the experimental structures than the theoretically 116
modeled ones). Under the influence of copper, there is a significant change in the length 117
of the imidazole ring bonds, which results in an increase in the HOMA and I5 indices. 118
Complexation of metals by ligand slightly changes the bond length of the triazene moiety 119
(Table 3). The complexation of cobalt with dacarbazine influences the change of 120
aromaticity of the imidazole ligand ring to a lesser extent than complexation of copper 121
(when comparing theoretical structures). A slight increase in the value of the I5 index and 122
a slight decrease in the value of the HOMA index were observed. The theoretical 123
structures of copper and cobalt complexes have similar bond lengths and angles. 124

It was observed that the complexation of dacarbazine with copper and cobalt slightly 125
changed the bond length of the N4-N5-N6 triazene moiety and the length of the N6-C5 126
and N6-C6 bonds (nitrogen N6 with methyl groups). The analysis of the NBO electronic 127
charge distribution (Table 4) showed that the values of the electronic charges on the 128
nitrogen atoms of the triazene group and the carbons of the methyl groups are similar in 129
the complexes and the ligand. 130

Table 4. NBO atomic charges calculated for dacarbazine and copper(II) and cobalt(II) complexes of dacarbazine   131

	DAC1	DAC2	Copper complex	Cobalt complex
O1	-0.605	-0.805	-0.607	-0.582
N1	-0.820	-0.627	-0.775	-0.764
C1	0.635	0.635	0.647	0.648
C2	0.021	0.013	0.008	-0.002
C3	0.283	0.307	0.314	0.321
N2	-0.555	-0.552	-0.514	-0.513
C4	0.219	0.220	0.279	0.276
N3	-0.444	-0.509	-0.518	-0.470
q_{ring}	-0.476	-0.521	-0.431	-0.388
N4	-0.346	-0.296	-0.343	-0.343
N5	-0.034	-0.047	-0.032	-0.031
N6	-0.248	-0.246	-0.215	0.213
C5	-0.390	-0.392	-0.390	-0.390
C6	-0.349	-0.349	-0.349	-0.349

On the other hand, the influence of metals on the distribution of electronic charge on the 132
imidazole ring of dacarbazine was observed. The electronic density around the carbon 133
atom labeled C2 and the nitrogen atom N3 increased in copper and cobalt complexes 134
compared to the ligand, while around the C3, C4 and N2 atoms the electronic density 135
decreased (Table 4). The effect of copper on the electronic charge distribution in the 136
imidazole ring of the ligand is greater than that of cobalt. The total electronic density of 137

the C-ring of the copper complex is greater than that of the cobalt complex. Studies of 4- 138
imidazole carboxylic acid complexes with 3d-transition metals (including copper and 139
cobalt) also showed that copper and cobalt had a stabilizing effect on the aromatic system 140
of the imidazole ring [38]. 141
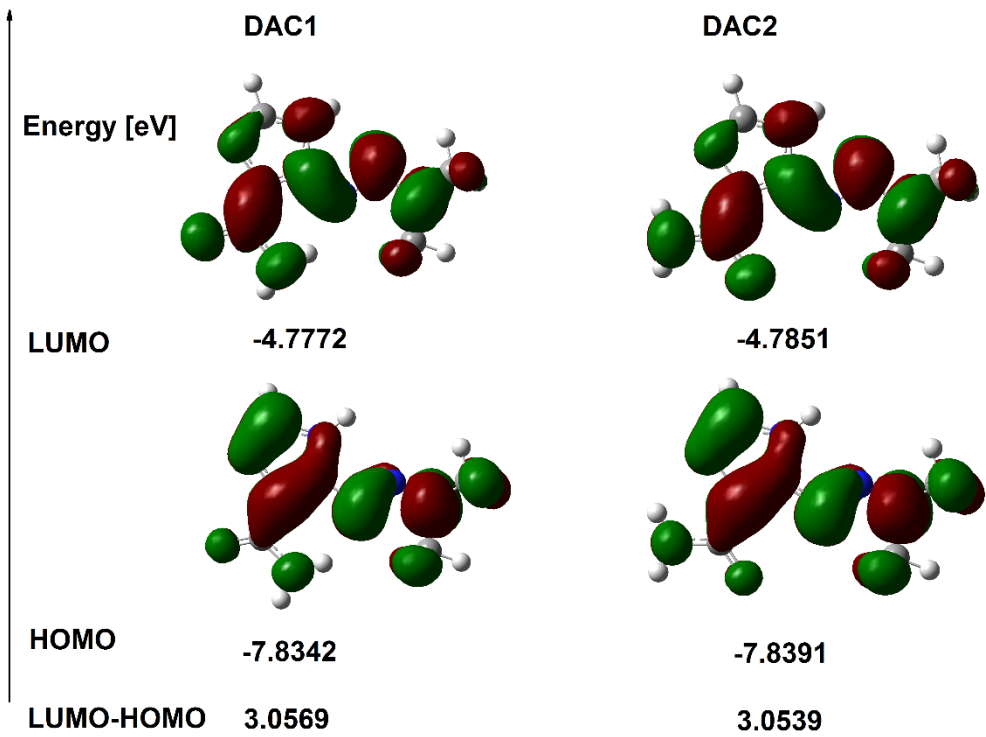
2.4. HOMO and LUMO orbitals

142

The energy values of the HOMO and LUMO orbitals for dacarbazine as well as 143
copper and cobalt complexes were calculated. The shapes of the orbitals are shown in 144
Figures 5 and 6, while in Table 5 the values of the energy of the orbitals and other 145
electronic parameters are gathered. The highest-occupied molecular orbital (HOMO) and 146
the lowest unoccupied molecular orbital (LUMO) play an important role in predicting 147
charge transfer in the molecule, chemical reactivity, bioactivity and compound stability 148
[36]. The shapes of the LUMO and HOMO molecular orbitals of the dacarbazine 149
complexes with copper and cobalt are shown in Figure 6. The energy values of the HOMO 150
and LUMO orbitals and the value of the energy difference between the HOMO-LUMO 151
levels for the studied compounds are presented in Table 5. The value of the HOMO-152
LUMO energy difference (Energy gap) for the copper complex is 0.3761 eV, and for the 153
cobalt complex it is 1.5894 eV and the values are lower than that one obtained for 154
dacarbazine (3.057 eV for DAC1). This indicates a decrease in kinetic stability and an 155
increase in the reactivity of the complexes towards the ligand. Other general reactivity 156
descriptors [40-41] such as ionization potential (I), electron affinity (A), electronegativity 157
(χ), chemical hardness (η), softness (e) and electrophilicity index (ω) calculated on the 158
basis of the Energy of HOMO and LUMO are summarized in Table 5. The data show that 159
the chemical hardness of the complexes is lower than that of the ligand. The 160
electrophilicity index (ω) provides information not only about the reactivity but also about 161
the toxicity of the molecule. This indicator is related to the stabilization of energy when 162
the system acquires an additional electrostatic charge from the environment and 163
quantifies the global electrophilic force of the molecule [42]. The electrophilicity index for 164
the copper complex is much higher than that of the free ligand (four times higher), while 165
for the cobalt complex it is twice as high as obtained for the ligand. 166

Table 5. The values of energy of HOMO and LUMO orbitals and other electronic paramaters calculated for dacarbazine 167
and copper(II) and cobalt(II) complexes of dacarbazine 168

	DAC1	DAC2	Copper complex	Cobalt complex
HOMO	-7,8342	-7,8391	-4,7827	-7,1092
LUMO	-4,7772	-4,7851	-4,4066	-5,5198
Energy Gap	3,057	3,054	0,3761	1,5894
Ionization potential	7,8342	7,8391	4,7827	7,1092
Electron Affinity	4,7772	4,7851	4,4066	5,5198
Electronegativity	6,3057	6,3121	4,59465	6,3145
Chemical potential	-6,3057	-6,3121	-4,59465	-6,3145
Chemical hardness	1,5285	1,527	0,18805	0,7947
Chemical softness	0,327118	0,327439	2,658867	0,629168

| Electrophilicity index | 13,00682 | 13,04604 | 56,13084 | 25,08677 |

169

DAC1   DAC2

Energy [eV]

LUMO   -4.7772   -4.7851

HOMO   -7.8342   -7.8391

LUMO-HOMO   3.0569   3.0539

170

Figure 5. HOMO and LUMO orbitals of dacarbazine   171

Copper complex   Cobalt complex

Energy [eV]

LUMO   -4.7772   -4.7851

HOMO   -4.4066   -5.5198

LUMO-HOMO   0.3761   1.5894
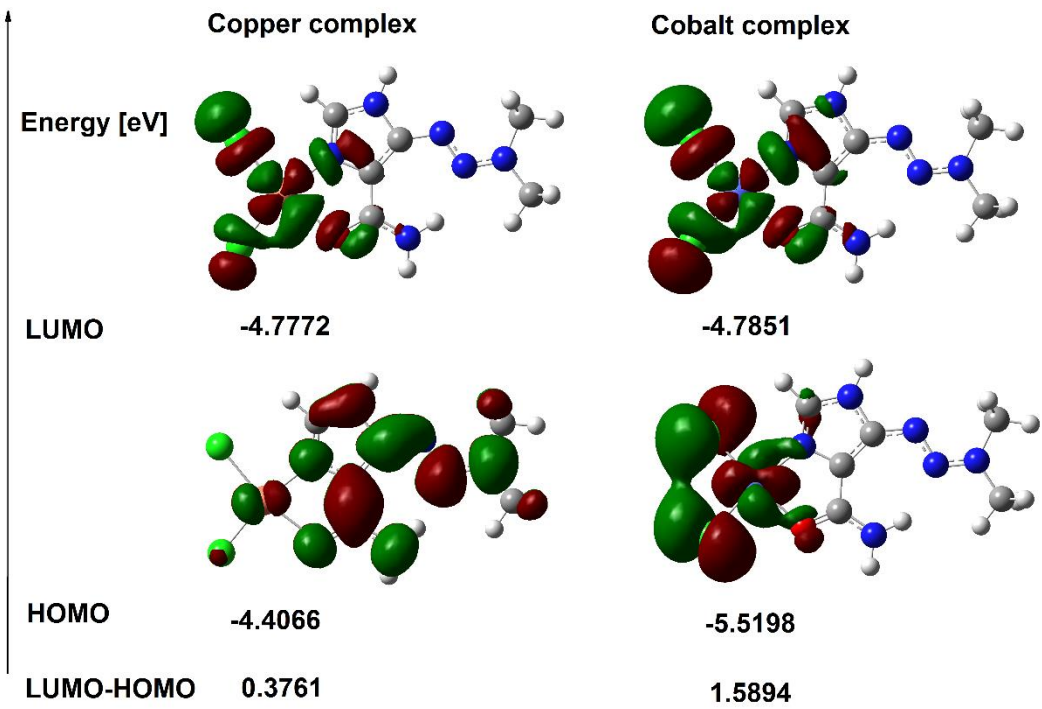
172

Figure 6. HOMO and LUMO orbitals of copper and cobalt complexes with dacarbazine   173

2.5.   Docking studies

174

Comparing the average number of hydrogen bonds formed with the B-DNA structure, it was observed that the number of H-Bonds does not change significantly in the case of decarbazine metal complexes compared to ligands. The obtained results indicate that the significant decrease (~4 kcal/M) in the free energy of binding the complexes with B-DNA is not due to formed hydrogen bonds (Fig 7). We conclude that formation of the complex cause favorable changes occur in the distribution of the electronic charge.   These changes in the electron density distribution affect the affinity to biological macromolecules like DNA. The tested compounds had an entropy value of S = 13.75 kcal / mol and an internal energy with values Dac1 (-4.37 kcal/mol), Dac2 (-4.26 kcal/mol), Cu-DAC (-8.13 kcal / mol), Co-DAC (-8.19 kcal/mol) respectively (Table 6). The most energetically advantageous complexes with DNA formed two hydrogen bonds with thymine (Fig. 8). In the case of constant inhibition, the value for metal complexes decreased by more than 1000-fold, and the free binding energy decreased by about 4 kcal / mol.

175
176
177
178
179
180
181
182
183
184
185
186
187
188

Table 6. Molecular docking analysis results

189

|	Free energy of binding (kcal/ mol)	Inhibition constant (μM)	Intermolecular energy	Torsional energy	Unbound extended energy	Interacting residues (H-Bonds) and distance [Å]	Reference RMSD
DAC 1	-5.17	163	-5.99	0.82	-0.38	N1-THY B:19 (1.92) N2-THY A:7 (2.11)	25.45
DAC 2	-5.13	173.91	-5.95	0.82	-0.37	N1-THY B:19 (1.96) N2:THY A:7 (2.11)	25.43
Cu-DAC	-9.31	0.15106	-10.40	+1.10	-0.63	N1-THY:A8 (2.19) N2-THY A:7 (1.86)	25.26
Co-DAC	-9.33	0.14391	-10.43	+1.10	-0.56	N2-THY A:7 (1.86) N1-THY B:19 (1.87)	26.06

190
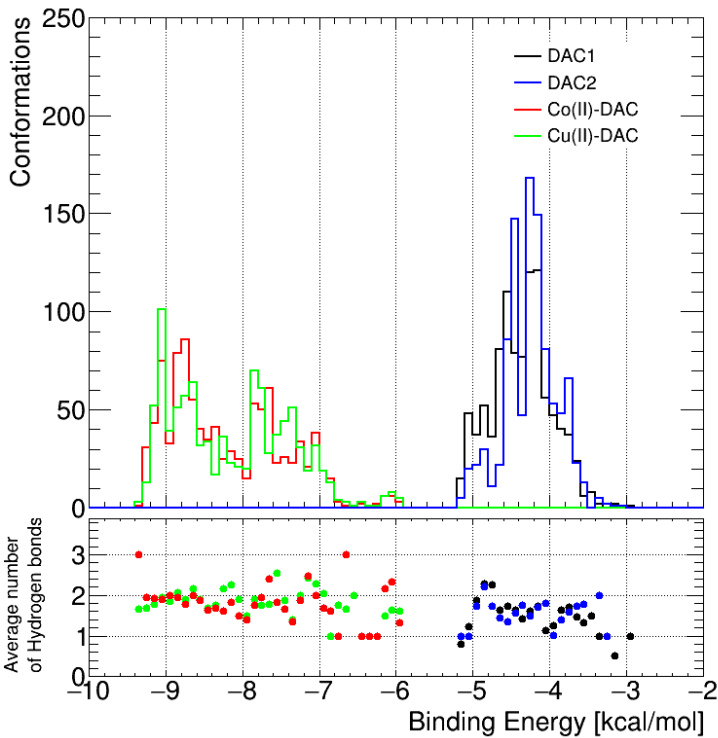
Figure 7. (Upper) Representation of number of conformations formed by both ligand conformers (DAC1,DAC2) and   192
metal complexes Co(II)-DAC and Cu(II)-DAC. (Lower) Average number of hydrogen bonds formed in complexes and   193
ligands and free binding energy.   194

In Ahmad & Ahmad studies, binding constant (Kb) was 7,89 x 10^4 M -1 in   195
experimental isothermal titration calorimetry of ct-DNA-DAC, and Kb = 6.99 × 10^4 M-1 in   196
docking studies for B-DNA-DAC [43]. Dacarbazine–ctDNA binding energy obtained from   197
ITC experiments was –5.49 kcal/mol and it is comparable with minimized free energy of   198
DAC–DNA obtained in docking studies (-5.35 kcal/mol). The most favorable interactions   199
were found in the A-T residue of the minor DNA groove and hydrogen bonding and van   200
der Waals interactions likely play a major role in these interactions. Previous research   201
described by Wang et al. [44] obtained by atomic force microscopy and nanostructural   202
image of DAC-DNA complexes indicate interaction at some specific site of the DNA   203
sequence without intercalation. Additional, DAC shows poor binding affinity to ssDNA   204
[44]. Based on cyclic voltammetry,   differential pulse voltammetry studies and using   205
spectroscopic methods performed by Radi et al, it has been concluded that decarbazine   206
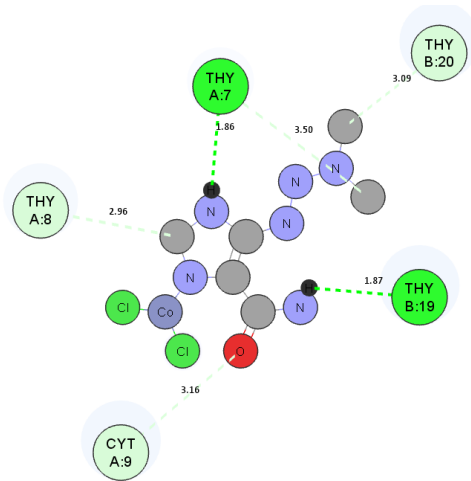binds to double-stranded DNA by combined effect of intercalation and electrostatic   207
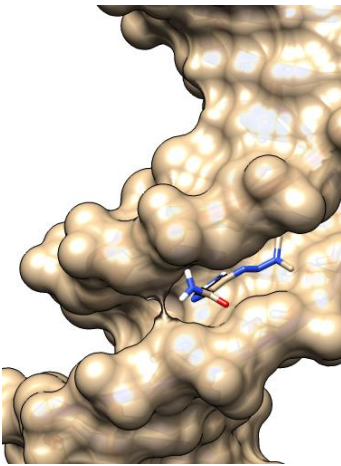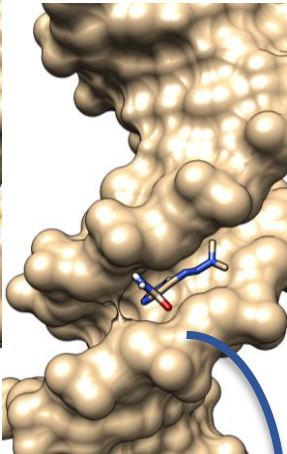interactions [46].   208
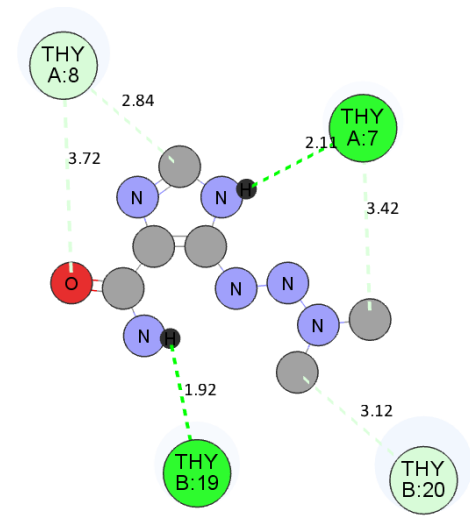
DAC1

DAC2

Cu-DAC

Co-DAC
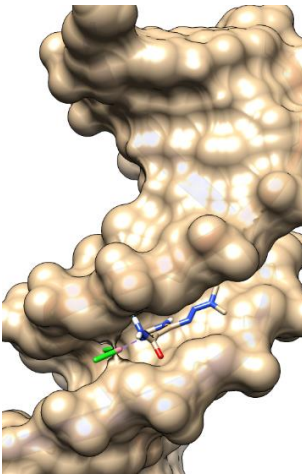
209
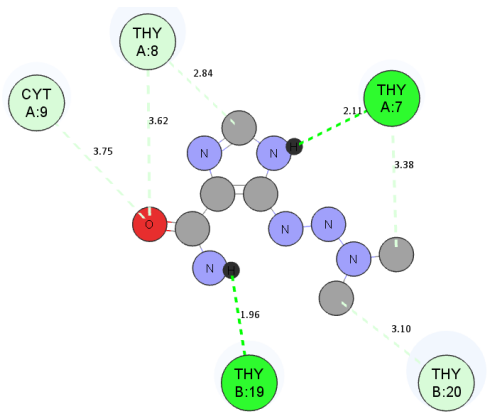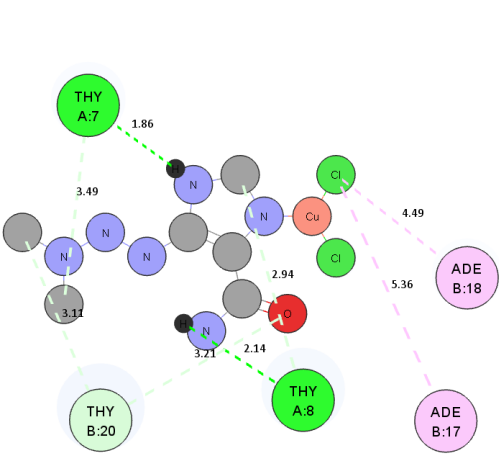
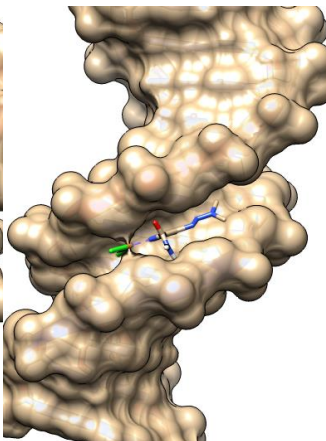

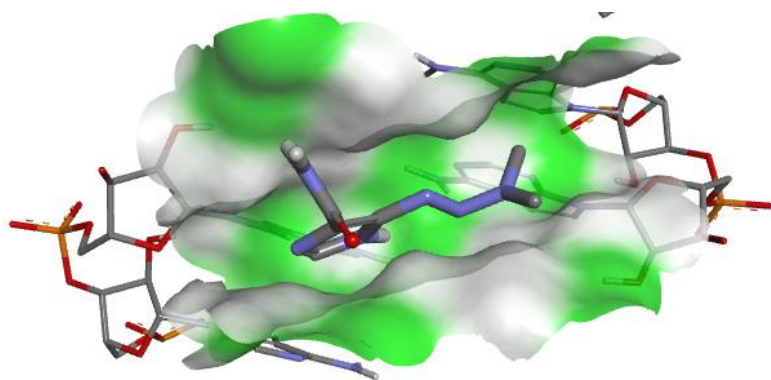**DAC1**   **DAC2**   **Co-DAC**   **Cu-DAC**

210

Figure 8. Best docking poses of decarbazine and complexes with B-DNA structure (Upper) in 2D with hydrogen bonds   211
(green), Van der Waals (light green) and Pi-Alkyl (pink) interactions. (Lower) 3D visualization of location in minor   212
groove of DNA.   213

Temerk & Ibrahim [46] describes that both DAC and DAC-Cu (II) complex   214
intercalate with base stacking of dsDNA, independent of ionic strength. In contrast, the   215
interaction of a DAC with ssDNA, which is negatively charged, is electrostatic attractions.   216
However, in the presence of Cu (II), these interactions are much stronger. Values of   217
standard Gibbs free energy ($-\Delta G\circ$) in 278 K for DAC-ssDNA is 28.74 kJ/M (6.87 kcal/M)   218
and for DAC-Cu(II)-ssDNA is 29.98 kJ/M (7.17 kcal/M) with enthalpy $\Delta H\circ$ = 21.98 kJ/M   219
and 22.29 kJ/M respectively. For comparison $-\Delta G\circ$ for DAC-dsDNA is 25.75 kJ/M and   220
27.55 kJ/Mol for DAC-Cu-dsDNA [46].   221

The presented results indicate the formation of beneficial interactions and   222
changes in the distribution of the electronic charge in decarbazine complexes with copper   223
and cobalt, which in turn may enhance the interaction with macromolecules such as DNA.   224

2.6. Thermogravimetric study   225

Thermogravimetric curves of dacarbazine and its metal complexes with copper   226
(II) and cobalt (II) were shown in Fig. 9. Dacarbazine underwent immediate   227
decomposition above 205oC. Rapid mass loss observed on the TG curve was accompanied   228
by narrow signal on the DTG curve. In the first stage of thermal decomposition of   229
dacarbazine (in the range of 205-210oC) the 50% loss in weight occurred. The mid weight   230
loss was due to degradation of triazene group and thermal dissociation of the amide   231
group. The second stage of thermal decomposition of decarbazine was less rapid (above   232
201oC) - the imidazole ring and C=O group totally decomposed and the total mass loss   233
was at 675oC (Table 7).   234
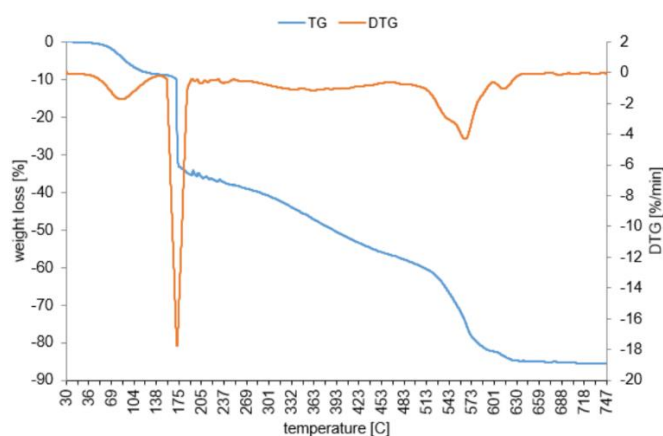
A
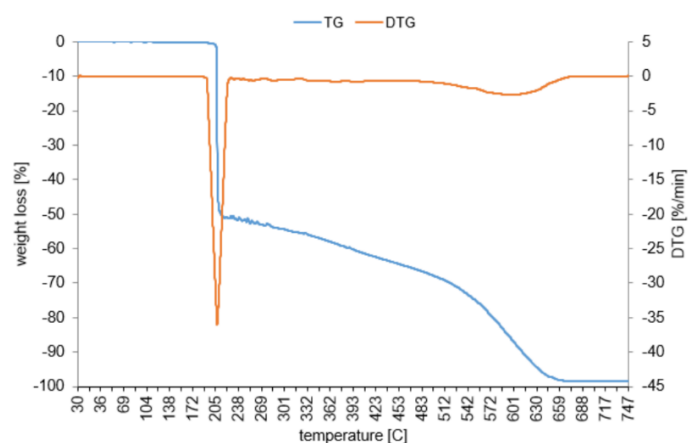
B
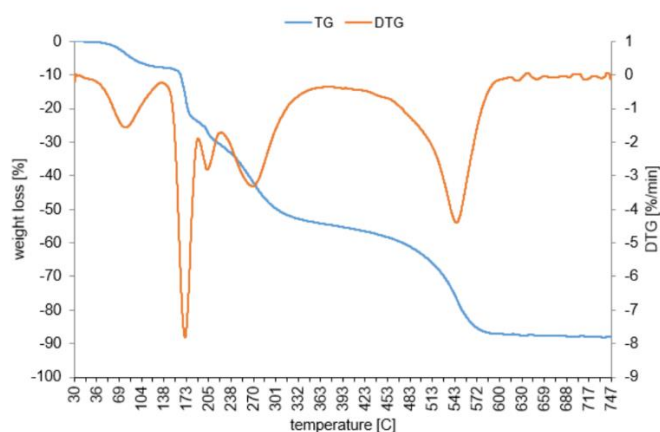
C

Figure 9. TG/DTG curves of dacarbazine (A), cobalt (B) and copper (C) complexes   235

In the first stage of thermal decomposition of copper (II) and cobalt (II) complexes of   236
dacarbazine the process of methanol desolvation occurred. Cobalt complex totally lost   237
methanol (1.75 mole of CH_3OH) in the range of 60-120°C, and copper complex (1.5 mole   238
of CH_3OH) in the range of 60-110°C. The thermal decomposition of cobalt compound   239
started at 175°C (at much lower temperature than decarbazine). The first stage of   240

decomposition was as rapid as it was in the case of ligand (with 33% loss in weight). The   241
second stage of decomposition ran gently until achievement the 540°C, and then the rapid   242
mass loss occurred. The TG curve possessed similar shape as TG curve of decarbazine. In   243
the 630°C the cobalt complex totally decomposed to CoO.   244

Table 7. The result s of thermal decomposition of dacarbazine and their complexes with cobalt and copper   245

Compound	Range of decomposition	Weight loss [%]		Products of decomposition
		Calcd.	found	
Dacarbazine	205-210	47.70	48.50	Imidazole +CO
	210-660	100	100	-
$CoCl_2(Dac)_2*1.75CH_3OH$	60-120	10.19	10.34	$CoCl_2(Dac)_2$
	175-630	86.38	85.61	CoO
$CuCl_2(Dac)_2*1.5CH_3OH$	60-110	8.78	8.39	$CuCl_2(Dac)_2$
	160-580	85.40	87.16	CuO

246

At the beginning of the thermal decomposition of copper (II) complex of   247
dacarbazine the methanol desolvation occurred. Next the thermal decomposition of   248
complex started at about 160°C (slightly lower temperature than in the case of   249
dacarbazine). During the thermal decomposition of copper complex no stable   250
intermediate products were observed (similarly as in the case of cobalt complex). Above   251
580°C the final product of decomposition CuO occurred. Comparing the curves of thermal   252
decomposition of studied compounds it appeared that complexes of dacarbazine were   253
less stable than ligand alone. The thermal decomposition of cobalt and copper complexes   254
started at the temperature of 35 and 50 degrees lower than ligand, respectively. Cobalt   255
complex of dacarbazine was more thermal stable than copper complex.   256

3. Conclusion   257

The spectroscopic IR and NMR studies revealed that dacarbazine coordinates   258
metal cations (cobalt (II) and copper (II)) through the oxygen atom of carbonyl group   259
and nitrogen atom from the imidazole ring. It was stated on the basis of significant shifts   260
of bands assigned to the vibrations of the aforementioned groups from the infrared   261
spectra and chemical shifts of protons from the 1HNMR spectra (changes in the electronic   262
charge density under the influence of complexation). The thermal analysis showed that   263
cobalt (II) and copper (II) complexes of dacarbazine were less stable than ligand. Cobalt   264
complex of dacarbazine was more thermal stable than copper complex.   265

Based on the literature data (X-ray diffraction) and spectroscopic data, the   266
theoretical structures of the complexes were modeled. Experimentally determined and   267
theoretically calculated structures were compared. For the modeled structures, the   268
distribution of electronic charge, aromaticity and energies of the HOMO and LUMO   269
orbitals were calculated. This allowed the assessment of the effect of complexation with   270
copper and cobalt on the stabilization of the aromatic system and the reactivity of the   271
investigated complexes. Complexation with copper and cobalt changes the electronic   272

charge distribution of dacarbazine. The aromatic system of dacarbazine is stabilized 273
(aromaticity indexes increase) due to metal complexation. The values of the calculated 274
energy of the HOMO and LUMO orbitals indicate an increase in the reactivity of the 275
dacarbazine molecule after complexation. This has a significant impact on the biological 276
activity of these substances. 277

278

Author Contributions: Conceptualization, G.S., M.K., R. Ł., methodology, G.S., M.K., 279
validation, W.L., R.Ł..; formal analysis, A.A., M.M., M.K., G.Ś., M.S., investigation, W.L., 280
R.Ł.; writing—original draft preparation, G,Ś., M.K., R.Ś, A.G., M.M., visualization, G.Ś., 281
A.G., A.A.; supervision, G. Ś..; project administration, W.L. 282

Conflicts of interest 286
No potential conflict of interest was reported by the authors. 287

References 288

1. Serrone, L.; Zeuli, M.; Sega, F.M.; Cognetti, F. Dacarbazine-based chemotherapy for metastatic melanoma: Thirty-year experience 289
   overview. J. Exp. Clin. Cancer Res. **2000**, 19(1), 21-34. 290

2. Reid, J.M.; Kuffel, M.J.; Miller, J.K.; Rios, R.; Ammes, M.M. Metabolic activation of dacarbazine by human cytochromes p450: the 291
   role of CYP1A1, CYP1A2e CYP2E1. Clin. Cancer Res. **1999**, 5, 2192–2197. 292

3. Nussbaumera, S.; Bonnabry, P.; Veuthey, J.L. Fleury-Souverain S. Analysis of anticancer drugs: A review. Talanta 293
   2011, 85, 2265–2289. 294

4. Moody, C.L.; Wheelhouse, R.T. The Medicinal Chemistry of Imidazotetrazine Prodrugs. Pharmaceuticals **2014**, 7, 797-838. 295

5. Bonmassar, L.; Marchesi, F.; Pascale, E.; Franzese, O.; Margison, G.P.; Bianchi, A.; D'Atri, S.; Bernardini, S.; Lattuada, D.; 296
   Bonmassar, E.; Aquino, A. Triazene compounds in the treatment of acute myeloid leukemia: a short review and a case report. 297
   Curr. Med. Chem. **2013**, 20, 2389-2401. 298

6. Marchesi, F.; Turriziani, M.; Tortorelli, G.; Avvisati, G.; Torino, F.; Vecchis, L.D. Triazene compounds: mechanism of action and 299
   related DNA repair systems. Pharmacol. Res. **2007,** 56, 275–287. 300

7. Pourahmad, J.; Amirmostofian, M.; Kobarfard, F.; Shahraki, J. Biological reactive intermediates that mediate dacarbazine cyto- 301
   toxicity. Cancer Chemother. Pharmacol. **2009,** 65, 89–96. 302

8. Hayward, I.P.; Parson, P.G. Epigenetic effects of the methylating agent 5-(3-dimethyl-1-triazeno)-imidazole-4-carboxamide in 303
   human melanoma cells. Aust. J. Exp. Biol. Med. Sci. **1984,** 62, 597–606. 304

9. Al-Qatati, A.; Aliwaini, S. Combined pitavastatin and dacarbazine treatment activates apoptosis and autophagy resulting in 305
   synergistic cytotoxicity in melanoma cells. Oncol. Lett. **2017,** 14, 7993-7999. 306

10. Naserian, M.; Ramazani, E.; Iranshahi, M.; Tayarani-Najaran, Z. The Role of SAPK/JNK pathway in the synergistic effects of 307
    metformin and dacarbazine on apoptosis in Raji and Ramos lymphoma cells. **2018**, 11(4), 336-342. 308

11. Finotello, R.; Stefanello, D.; Zini, E.; Marconato, L. Comparison of doxorubicin–cyclophosphamide with doxorubicin–dacarba- 309
    zine for the adjuvant treatment of canine hemangiosarcoma. Vet. Comp. Oncol. **2015**, 15, 25-35. 310

12. Song, M.; Zhang, R.; Wang, X. Nano-titanium dioxide enhanced biosensing of the interaction of dacarbazine with DNA and 311
    DNA bases. Mater Lett. **2006,** 60, 2143-2147. 312

13. Shen, Q.; Wang, X.; Fu, D. The amplification effect of functionalized gold nanopar-ticles on the binding of anticancer drug 313
    dacarbazine to DNA and DNA bases. Appl. Surf. Sci. **2008**, 255, 577-580. 314

14. Matejczyk, M.;   Świsłocka, R.; Golonko, A.; Lewandowski, W.; Hawrylik, E. Cytotoxic, genotoxic and antimicrobial activity of caffeic and rosmarinic acids and their lithium, sodium and potassium salts as potential anticancer compounds.   Adv. Med. Sci. **2008**, 63(1), 14-21.

15. Jabłońska-Trypuć, A.; Świderski, G.; Krętowski, R.; Lewandowski, W. Newly synthesized doxorubicin complexes with selected metals - Synthesis, structure and anti-breast cancer activity. Molecules **2017,** 22(7) 1106.

16. Trynda – Lemiesz, L.; Śliwińska-Hill, U. Kompleksy metali w terapii nowotworowej. Teraźniejszość i przyszłość, J. Oncol. **2011**, 61(5), 465-474.

17. Kumari, T.; Shukla, J.; Joshin, S. Study on the complex formation and anticancer effect of complex, zinc(II)-dacarbazine. Int. J. Chem. Sci. **2011**, 9(4), 1751-1762.

18.   Shukla, J.; Pitre, K.S. Role of bio-metal Fe(III) in anticancer effect of dacarbazine. Indian J. Physiol. Pharmacol. **1998**, 42(2), 223-230.

19. Yassien, T.; Hossieny, I. Binding mode and thermodynamic studies on the interaction of the anticancer drug dacarbazine and dacarbazine–Cu(II) complex with single and double stranded DNA. J. Pharm. Biomed. Anal. **2014**, 95, 26-33.

20. Lewandowski, W.; Kalinowska, M.; Lewandowska, H. The influence of metals on the electronic system of biologically important ligands, Spectroscopic study of benzoates, salicylates, nicotinates and isoorates. Review. J. Inorg. Biochem. **2005**, 99, 1407-1423.

21. Koczoń, P.; Hrynaszkiewicz, T.; Świsłocka, R.; Samsonowicz, M.; Lewandowski, W. Spectroscopic (Raman, FT-IR and NMR) study of alkaline metal nicotinates and isonicotinates.   Vib. Spectrosc. **2003**, 33, 215-222.

22. Lewandowska, M.; Janowski, A.; Lewandowski, W. Spectroscopic Investigations on Lanthanide Complexes with Salicylic Acid. Can. J. Spectr. **1984**, 29, 87-92.

23. Lewandowski, W.; Kalinowska, M.; Lewandowska, H. The influence of halogens on the electronic system of biologically im-portant ligands. Spectroscopic study of halogenobenzoic acids, halogenobenzoates and 5-halogenouracils. Review. Inorg. Chim. Acta. **2005**, 358, 2155-2166.

24. Koczoń, P.; Piekut, J.; Borawska, M.; Lewandowski, W. Vibrational structure and antimicrobial activity of selected isonicotinates, potassium picolinate and nicotinate. J. Mol. Struct. **2003**, 651-653, 651-656.

25. Kalinowska, M.; Borawska, M.; Świsłocka, R.; Piekut, J.; Lewandowski, W. Spectroscopic (IR, Raman, UV, ^{1}H and ^{13}C NMR) and microbiological studies of Fe(III), Ni(II), Cu(II), Zn(II) and Ag(I) picolinates. J. Mol. Struct. **2007**, 834-836, 419-425.

26. Świderski, G.; Świsłocka, R.; Łyszczek, R.; Wojtulewski, S.; Samsonowicz, M.; Lewandowski, W. Thermal, spectroscopic, X-ray and theoretical studies of metal complexes (sodium, manganese, copper, nickel, cobalt and zinc) with pyrimidine-5-carboxylic and pyrimidine-2-carboxylic acids. J. Therm. Anal. Calorim. **2019**, 138(4), 2813-2837.

27. Frisch, M.J.; at al. , Gaussian, Inc., Wallingford, CT; 2008.

28. Krygowski, T.M.; Cyrański, M. Separation of the energetic and geometric contributions to the aromaticity. Part IV. A general model for thep-electron systems. Tetrahedron **1996**, 52, 10255-10264.

29. Bird, C. A new aromaticity index and its application to fivemembered ring heterocycles. Tetrahedron **1985,** 41, 1409-1414.

30. Weinhold, F.; Landis, C.R. Natural bond orbitals and extensions of localized bonding concepts. Chem. Educ. Res. Pract. **2001**, 2(2), 91-104.

31. Humphrey, W.; Dalke, A.; Schulten, K. VMD: Visual molecular dynamics. J. Mol. Graph. **1996**, 14, 33–38.

32. Morris, G.M.; Huey, R.; Lindstrom, W.; Sanner, M.F.; Belew, R.K.; Goodsell, D.S.; Olson, A.J. Software news and updates AutoDock4 and AutoDockTools4: Automated docking with selective receptor flexibility. J. Comput. Chem. **2009**, 30, 2785–2791.

33. Systèmes D. BIOVIA Discovery Studio. 2016.

34. Pettersen, E.F.; Goodard, T.D.; Huang, C.C.; Couch, G.S.; Greenblatt, D.M.; Meng, E.C.; Ferrin, T.E. UCSF Chimera - A visualization system for exploratory research and analysis. J. Comput. Chem. **2004**, 25, 1605–1612.

35. Gunasekaran, S.; Kumaresan, S.; Arunbalaji, R.; Anand, G.; Srinivasan, S. Density functional theory study of vibrational spectra, and assignment of fundamental modes of dacarbazine.   J. Chem. Sci. **2008**, 120(3), 315-324.

36. Freeman, H.C.; Hutchinson, N.D. The crystal structure of the anti-tumor agent 5-(3, 3-dimethyl-1-triazenyl) imidazole-4-carbox-   358
     amide, Acta Crystall. Sec. B **1979**, 35(9), 2051-2054.   359

37. Freeman, H.C.; Hutchinson, N.D. The crystal structures of two copper(II) complexes of the antitumor agent 5-(3, 3-dimethyl-1-   360
     triazenyl) imidazole-4-carboxamide, Acta Crystall. Sec. B **1979,** 35(9), 2045-2050.   361

38. Świderski, G.; Wilczewska, A.Z.; Świsłocka, R.; Kalinowska, M.; Lewandowski, W. Spectroscopic (IR, Raman, UV–Vis) study   362
     and thermal analysis of 3d-metal complexes with 4-imidazolecarboxylic acid. J. Therm. Anal. Calorim. **2018**, 134(1), 513-525.   363

39. Yousef, T.A.; El-Gammal, O.A.; Ahmed, S.F.; Abu El-Reash, G.M. Synthesis, biological and comparative DFT studies on Ni(II)   364
     complexes of NO and NOS donor ligands. Spectrochim. Acta A, **2015,** 135, 690–703.   365

40. Fukui, K. Role of frontier orbitals in chemical reactions. Science **1982**, 218, 747–754.   366

41. Parr, R.G.; Szentpály, L.V.; Liu, S. Electrophilicity Index. J. Am. Chem. Soc. **1999**, 121, 1922–1924.   367

42. Samsonowicz, M. Molecular structure of phenyl- and phenoxyacetic acids - spectroscopic and theoretical study.   368
     Spectrochim. Acta A. **2014,** 118, 1386–1425.   369

43. Ahmad, I.; Ahmad, M. Dacarbazine as a minor groove binder of DNA: Spectroscopic, biophysical and molecular docking studies.   370
     Int. J. Biol. Macromol. **2015,** 79, 193–200,   371

44. Wang, X.; Li, Y.; Gong S.; Fu, D. A spectroscopic study on the DNA binding behavior of the anticancer drug dacarbazine.   372
     Spectrosc. Lett. **2002,** 35, 751–756.   373

45. Radi, A.E.; Eissa, A.; Nassef, H.M. Voltammetric and spectroscopic studies on the binding of the antitumor drug dacarbazine   374
     with DNA. J. Electroanal. Chem. **2014**, 717–718, 24–28.   375

46. Temerk, Y.; Ibrahim, H. Binding mode and thermodynamic studies on the interaction of the anticancer drug dacarbazine and   376
     dacarbazine-Cu(II) complex with single and double stranded DNA. J. Pharm. Biomed. Anal. **2014,** 95, 26–33.   377

     378